Hindawi
Journal of Nanomaterials
Volume 2019, Article ID 4020762, 8 pages
https://doi.org/10.1155/2019/4020762

*Research Article*

# Electronic Structural and Optical Properties of Multilayer Blue Phosphorus: A First-Principle Study

**Bing Li, Ceng-Ceng Ren, Shu-Feng Zhang, Wei-Xiao Ji, Chang-Wen Zhang, Ping Li, and Pei-Ji Wang**

*School of Physics, University of Jinan, Jinan, Shandong 250022, China*

Correspondence should be addressed to Pei-Ji Wang; ss_wangpj@ujn.edu.cn

Received 31 May 2018; Revised 18 October 2018; Accepted 1 November 2018; Published 29 January 2019

Academic Editor: Achim Trampert



Using the density functional theory, we systematically calculated the stability, electronic, and optical properties of monolayer and multilayer blue phosphorus. The results show the structures are all dynamically stable, and the gaps decrease with an increase of the number of layers. An unexpected transformation from indirect to direct band gaps is also observed as the tensile strain increases. In addition, the optical properties indicate the optical absorption peak of the material is in the ultraviolet region.

## 1. Introduction

In recent years, the monolayer black phosphorus has been exfoliated named black phosphorene (BP) [1–7] and attracted tremendous attention due to its fascinating properties [8]. Compared with graphene, BP had a direct band gap and high carrier mobility, which would facilitate the application in optoelectronics. The band gap can be varied from 0.3 eV to 2.0 eV with the stripping of the monolayer black phosphorus [9]. Transport studies revealed high room temperature mobility ~1000 $cm^2 V^{-1} s^{-1}$ [10] and large on/off current ratio in the BP-based electronic device. BP had the corrugated in-plane lattice structure which led to interesting anisotropic behaviors in the electrical and optical responses.

By certain dislocation of constituent P atoms, the puckered structure of black phosphorus can be converted to a more symmetric buckled structure of another 2D allotrope, named blue phosphorus. Blue phosphorus has a hexagonal honeycomb lattice structure which is very different from BP. Blue phosphorus has been predicted through the ab initio density functional theory [11]; it displays a sizable fundamental indirect band gap [12, 13]. Through doping, adsorption, and functional group modification, scientists controlled the electronic properties of blue phosphorus materials and obtained a series of results. Sun et al. proposed that blue phosphorus band gap can be changed by modifying transitional atoms, and they also found blue phosphorus has a Dirac-cone by halogen modification; a linear relationship between energy and wave vector formed a Dirac cone near the Fermi level expressed as the relativistic particle behavior with zero effective mass and velocity close to the speed of light, which may be a potential Dirac material [14–19]. Zhu et al. revealed blue phosphorus oxide can be topological semiconductor materials by tunable strain [20]. The electronic band gap of the quasi-free-standing single-layer blue phosphorus, which was grown in tellurium functionalized Au(1 1 1), has been determined to be 1.10 eV by scanning tunneling spectroscopy measurement [21, 22]. Although the electronic structure of blue phosphorus has been extensively studied, optical properties are rarely involved. In addition, there are some unexplored issues in our knowledge which need us to continue in research.

In this study, we focus on the effect of the tensile strain and layers to the band gap, which rely on van der Waals (vdW) forces in multilayer blue phosphorus. These calculations indicated that the band gaps can be tuned effectively

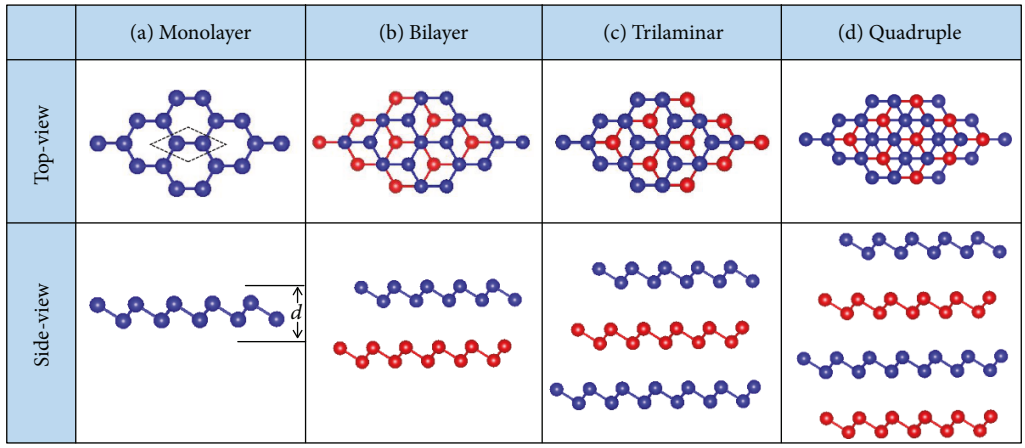


Figure 1: The top and side views of blue phosphorus (a) monolayer, (b) bilayer, (c) trilaminar, and (d) quadruple. In here, the blue color represents A stacked, and the red color is B stacked.

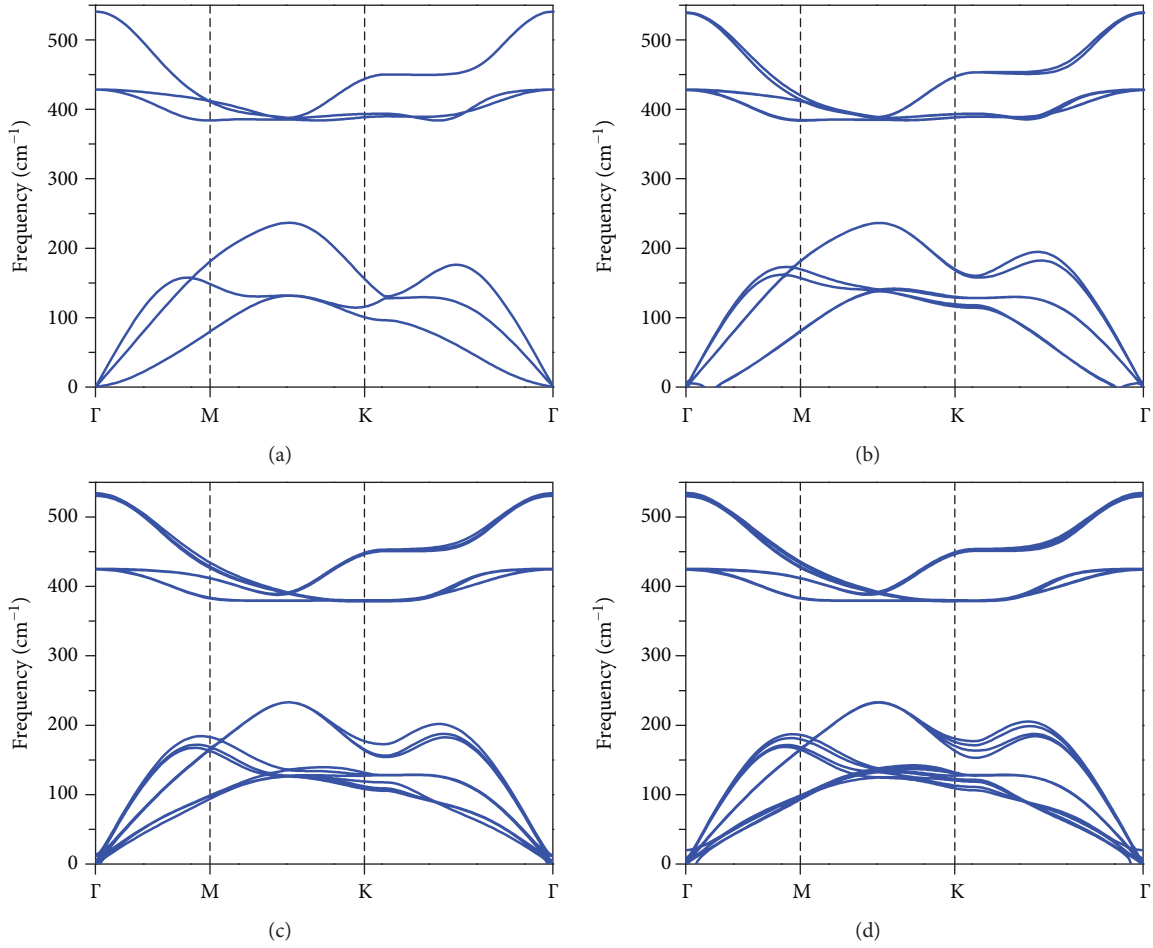


Figure 2: The vibration spectrum of (a) monolayer, (b) bilayer, (c) trilaminar, and (d) quadruple along the high-symmetric points in the BZ.

and have a transition from indirect to direct by the tensile strain. At the same time, the materials have a strong absorption in the ultraviolet range and intended to discover its potential applications in optoelectronic devices, and the underlying mechanism is analyzed.

## 2. Method

These first-principle calculations are performed through using the VASP [23, 24] code. The generalized gradient approximation (GGA) for the exchange and correlation

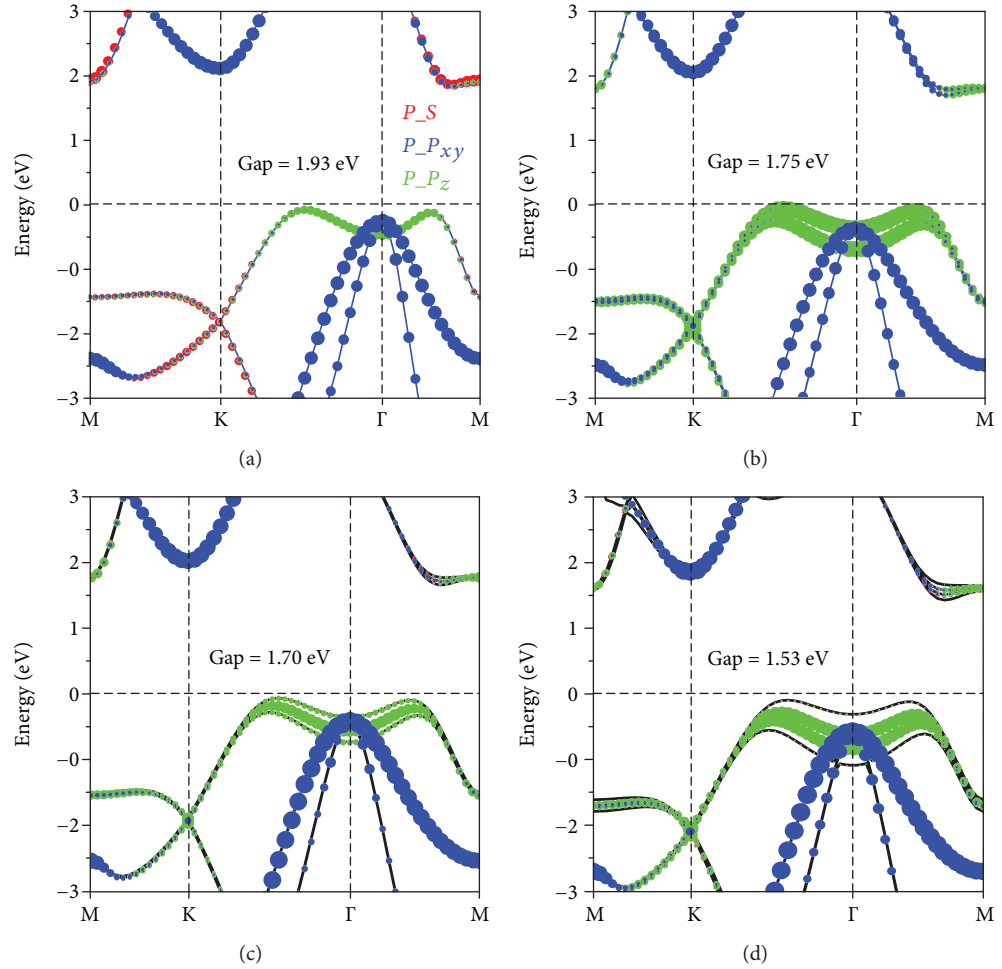


Figure 3: The electronic band structure of blue phosphorus (a) monolayer, (b) bilayer, (c) trilaminar, and (d) quadruple.

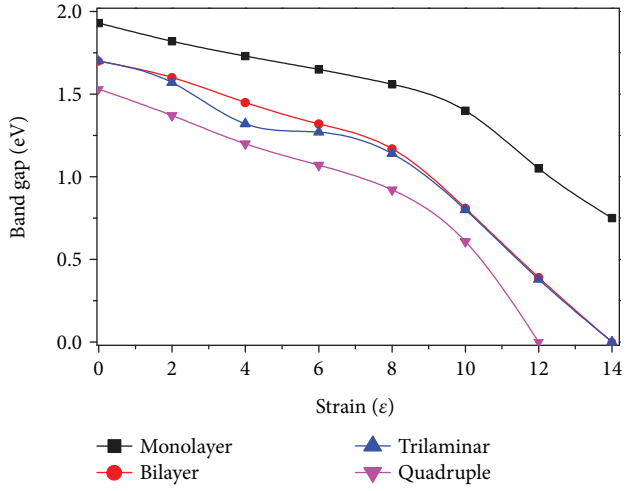


Figure 4: The band gap variation trend of blue phosphorus structures within the tensile strain.

potential, Perdew-Burke-Ernzerhof (PBE), the norm-conserving pseudopotentials [25, 26], and the projector augmented wave potential (PAW) [27] to treat the ion-electron interactions are used. To properly take into account the van der Waals (vdW) interactions in the structures, the DFT-D2 method was used throughout all the calculations [28, 29]. Similar methods to relax black phosphorus have been shown to produce results that closely match experimental data. The plane wave energy cutoff is set to 500 eV to ensure the convergence of total energy with the energy precision of $10^{-6}$ eV. The reciprocal space is sampled by a fine grid of $7 \times 7 \times 1$ $K$ point in the Brillouin zone (BZ). The conjugate-gradient method was used for geometrical optimization until the force on each atom was smaller than 0.02 eV/Å. The kinetic energy cutoff for wave function is set to be 500 eV. The phonon spectrum is calculated using a supercell approach within the PHONOPY code [30].

## 3. Result and Discussion

*3.1. Electronic Properties.* As shown in Figure 1(a), the lattice of monolayer blue phosphorus is a hexagonal honeycomb. In addition, there is a unit cell in black dashed frame and the side view shows that the structure is wrinkled. In Figures 1(b)–1(d), the first layer is named A which is

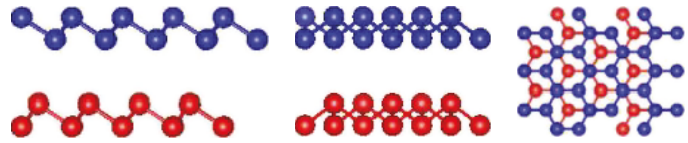

(a) $x$-direction (b) $y$-direction (c) $z$-direction

Figure 5: The unit cell to calculate optical properties and show the direction of light.

represented with color blue atoms and, in order to distinguish them, the second layer is named B which is represented with color red atoms. The lattice parameters of blue phosphorus are $a = b = 3.28$ Å, the height of the vacuum layer is at least 15 Å besides the distance of layers, and the bond length between two $P$ atoms is 2.265 Å.

From Figure 2, the dynamic stability is confirmed by the phonon spectrum calculated along the highly symmetric directions with zero strain, and the frequencies of all modes are positive over the whole Brillouin zone, indicating the structure is dynamically stable [31–40].

To evaluate the structural stability of the four structures, the binding energies are calculated as

$$E_b = E_f - N \cdot E_0, \tag{1}$$

where $E_f$ and $E_0$ are the energies of films and monolayer and $N$ is the number of layers. We calculated the binding energy of layers, $E_{\text{bilayer}}$, $E_{\text{trilaminar}}$, and $E_{\text{quadruple}}$ which are ~0.40 eV per P atom. We suggested that it is van der Waals interaction between layers, different from the strong orbital hybridization [41].

Figure 3 displays the electronic properties of multilayer blue phosphorus films. The band gaps of blue phosphorus are 1.93 eV (monolayer), 1.75 eV (bilayer), 1.70 eV (trilaminar), and 1.53 eV (quadruple) which are decreasing as the layers increase. The results indicate that the structures are all indirect band gap semiconductors. The conduction band minimum (CBM) of multilayer blue phosphorus films is between Γ and M, and the valence band maximum (VBM) of it is between K and Γ. Compared with Figure 3(a), $s$ reduces its effect while $p_{xy}$ and $p_z$ increase that the band is splitting at CBM; similarly, the band is also splitting near Γ in Figures 3(b)–3(d). The increasing layers added the number of band gaps near the Fermi level, the rule is $h = 2i$, $h$ is the number of band gap, and $i$ is the layer. Considering the above results, the top of the valence band will cross the Fermi surface and the material will change from a semiconductor to a metal as layers increase. The astonishing thing is that it has a Dirac cone at $K$ point which does not disappear as layers change, so blue phosphorus is also a potential choice for a Dirac material.

In order to discuss the effect of strain on the multilayer blue phosphorus band gaps, the 0~14% tensile strain to maintain all crystal symmetries and overall honeycomb-like structures were used. Here, the strain is defined as $\varepsilon = \Delta a/a_0$, where $a_0$ and $a = \Delta a + a_0$ are the lattice constants of the unstrained and strained cell, respectively.

In Figure 4, the results show that the band gaps decrease as the tensile strains increase showing the band variation trend of different layers of blue phosphorus in different tensile strains, in which band gaps will continue to decrease as tensile strains increase. For bilayer blue phosphorus, the VBM is located near the Fermi level and the CBM moves down continuously until crossing the Fermi level. Its band gap has a transition from indirect to direct within tensile strain $\varepsilon = 12\%$, while the CBM and VBM are at symmetry point Γ in which trilaminar and quadruple are within tensile strain $\varepsilon = 10\%$. From the results, the tensile strain can play an intensive role in the electronic structures of the multilayer blue phosphorus, so that it can be a potential choice of semiconductor switching to realize on/off within the tensile strain.

*3.2. Optical Properties.* The dielectric function is a function of the relationship between the energy band structure and optical properties of the reaction solids, which can be used to characterize the physical properties of semiconductor materials. The formula of complex dielectric function is expressed as

$$\varepsilon(\omega) = \varepsilon_1(\omega) + i\varepsilon_2(\omega), \tag{2}$$

where $\varepsilon_1(\omega)$ is the real part of the function, while $\varepsilon_2(\omega)$ is the imaginary part. The real part $\varepsilon_1(\omega)$ of the dielectric function can be calculated from the imaginary part $\varepsilon_2(\omega)$ by the Kramers–Kronig relationship, while the imaginary part $\varepsilon_2(\omega)$ has the following expression [42–44]:

$$\varepsilon_2(\omega) = \frac{4\pi^2}{m^2\omega^2} \sum_{V,C} \int_{\text{BZ}} d^3k \frac{2}{2\pi} |e \cdot M_{cv}(K)|^2 \times \delta[E_C(k) - E_V(k) - \hbar\omega]. \tag{3}$$

Herein, $\hbar = h/2\pi$, $m$ is the mass of free electrons, $e$ is the charge of free electrons, $\omega$ is the frequency of incident photons, $E_V$ and $E_C$ represent the conducting and valence bands, respectively, BZ represents the first Brillouin Zone, and $K$ is the reciprocal vector.

Blue phosphorus has different structures along the $x$ -direction and $y$-direction, so it is anisotropic in different directions. Moreover, as the number of layers increases, the optical properties also were calculated along the $z$-axis. It proves the structures of the material in different directions,

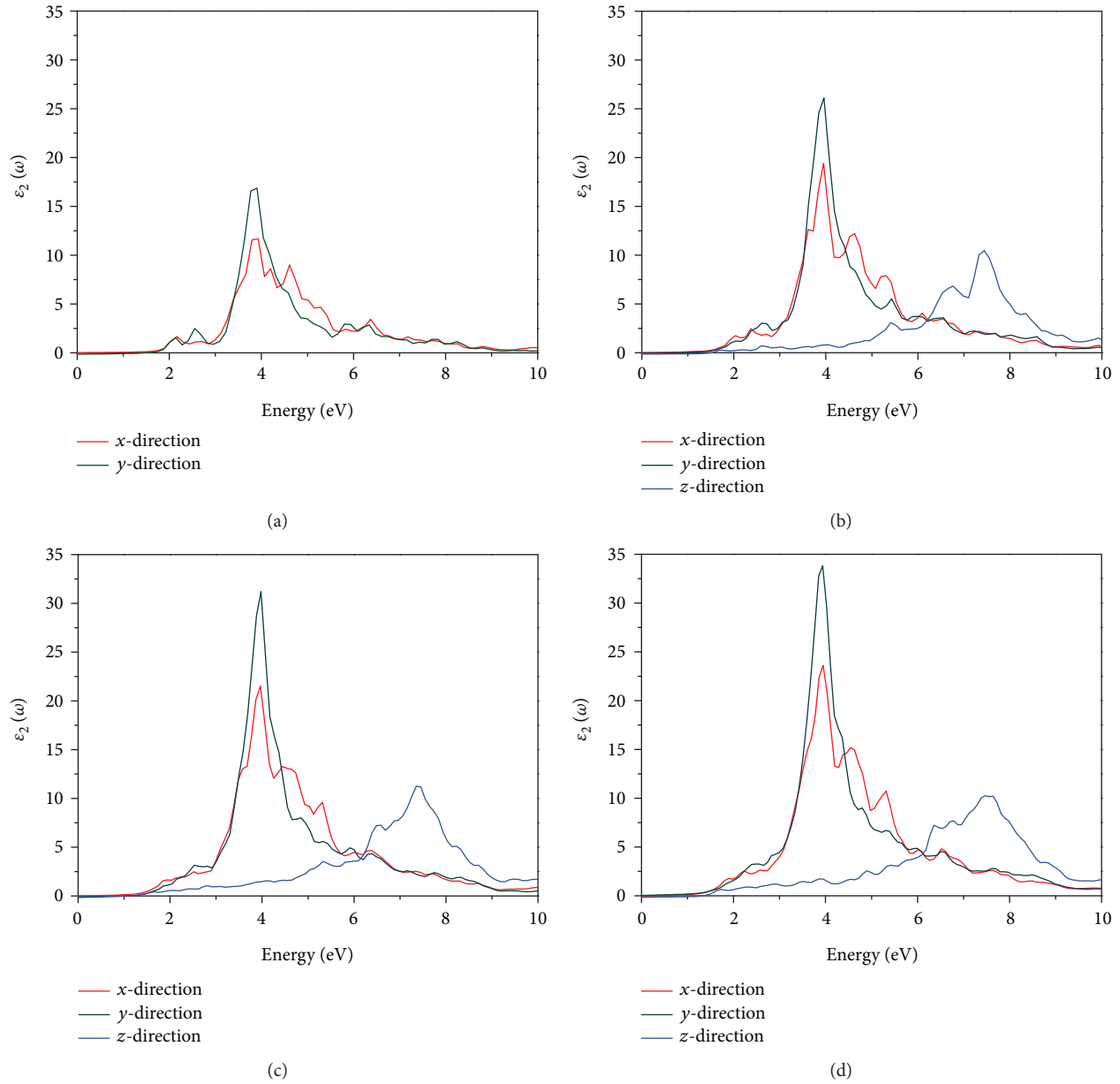


FIGURE 6: The imaginary part of the dielectric function of blue phosphorus $\varepsilon_2$ (a) monolayer, (b) bilayer, (c) trilaminar, and (d) quadruple. The red curve shows the optical properties of materials along the $x$-direction, the green curve shows those along the $y$-direction, and the blue curve shows those along the $z$-direction (along vacuum layer direction).

and the light runs perpendicular to the plane in Figure 5. We calculated the optical properties of the materials, and the results are presented in Figures 6 and 7.

From Figure 6, the results show that their peak intensity at ~4.0 eV in the $y$-direction is at its maximum in their structures, and besides, there are two lower peaks at ~2.1 and ~2.6 eV in Figure 6(a). Similarly, there is a peak at ~4.0 eV in the $x$-direction and two lower peaks at ~4.5 eV and ~5.3 eV in all structures. More than the monolayer, there is a peak at ~7.5 eV in the $z$-direction in four structures. There are many peaks in the range from 4.0 to 8.0 eV which mainly originates from the transition of the $p$ electrons, and it also causes changes in the main peaks of the dielectric function.

Next, we obtain the absorption coefficient $\alpha(\omega)$ from $\varepsilon_1(\omega)$ and $\varepsilon_2(\omega)$, and the absorption area [45, 46] is expressed by

$$I(\omega) = \sqrt{2}\omega\left[\sqrt{\varepsilon_1^2(\omega) - \varepsilon_2^2(\omega)} - \varepsilon_1(\omega)\right]^{1/2}, \quad \lambda = h \cdot C/E. \tag{4}$$

In Figure 7, the optical absorption spectrums show that absorption curves almost start at ~2.0 eV. Unlike another absorption curves, it has absorption peaks at ~2.1 and ~2.6 eV in the $y$-direction which represents a monolayer that can absorb green light in the $y$-direction rather than the $x$

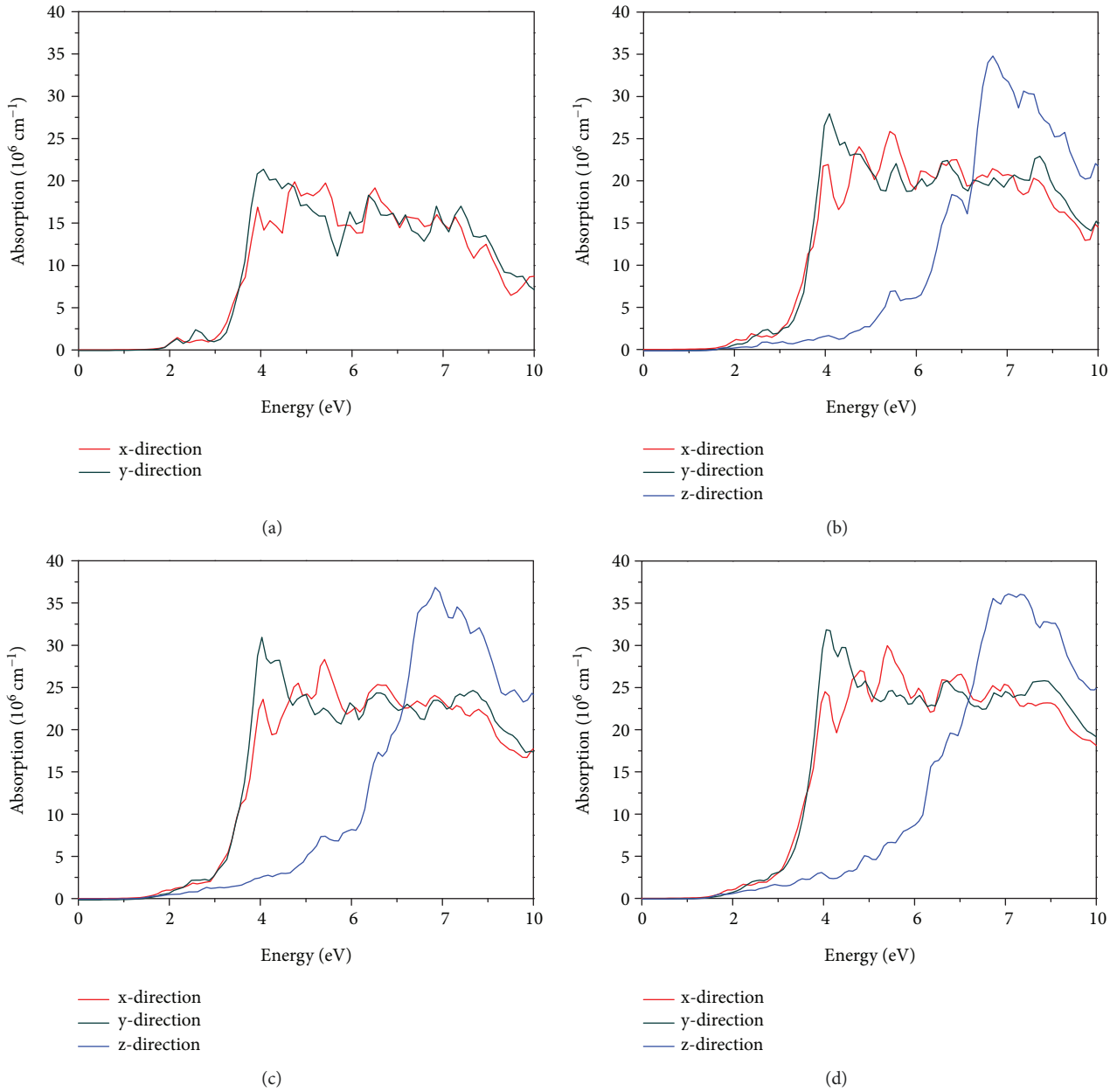


Figure 7: The optical absorption spectrum of blue phosphorus (a) monolayer, (b) bilayer, (c) trilaminar, and (d) quadruple. The red curve shows the optical properties of materials along the $x$-direction, the green curve shows those along the $y$-direction, and the blue curve shows those along the $z$-direction (along vacuum layer direction).

-direction in Figure 7(a), and this peak will disappear as the number of layers increases. Besides, the absorption coefficients all have an absorption peak at ~4.0 eV increasing up to the order of $10^7$ cm$^{-1}$, and the value of coefficients is enhancing as layers increase. In the $x$-direction and $y$-direction, there are multiple absorption peaks in the range of 4.0 eV to 8.0 eV and then the absorption coefficients will decrease as energies continue to enhance. Layers increasing caused the absorption in the $z$-direction, compared with the $x$-direction and $y$-direction; the absorption coefficient has a peak at ~8.0 eV. In conclusion, we found that the energy of peaks is almost always greater than 3.0 eV so that the material is mainly absorbed by ultraviolet light.

From the results, we believe that along the same direction of light irradiation, the increasing of layers can hardly affect the absorption wavelength of light, but the absorption coefficients will increase. Multilayer blue phosphorus structures present significant absorption in the range of ultraviolet light, which can be attractive for efficient light harvesting in optoelectronics instruments.

## 4. Conclusion

To summarize, we systematically investigated the structural, electronic, and optical properties of multilayer phosphorus via DFT computations. Pure blue phosphorus is an

indirect band gap semiconductor, and the band gaps gradually become smaller as the layers increase. The method of tensile strain is applied to make it become a direct band gap and implement the band gaps of the opening and closing. In addition, the monolayer blue phosphorus can absorb the green light by calculating the optical properties and multilayer blue phosphorus structures become the only absorption ultraviolet ray as the layers increase. Overall, our results have a research value in electronics and optoelectronics devices.

## Data Availability

The data used to support the findings of this study are available from the corresponding author upon request.

## Conflicts of Interest

The authors declare that they have no conflicts of interest.

## Acknowledgments

This work was supported by the National Natural Science Foundation of China (Grant nos. 61571210, 61172028, and 11434006).

## Supplementary Materials

Table 1: the variation of the lattice parameter with biaxial tensile strain, $\varepsilon = \Delta a/a_0$, where $a_0$ and $a = \Delta a + a_0$ are the lattice constants of the unstrained and strained cell. *(Supplementary Materials)*

## References

[1] H. Liu, A. T. Neal, Z. Zhu et al., "Phosphorene: an unexplored 2D semiconductor with a high hole mobility," *ACS Nano*, vol. 8, no. 4, pp. 4033–4041, 2014.

[2] Y.-C. Lin, D. O. Dumcenco, Y.-S. Huang, and K. Suenaga, "Atomic mechanism of the semiconducting-to-metallic phase transition in single-layered $MoS_2$," *Nature Nanotechnology*, vol. 9, no. 5, pp. 391–396, 2014.

[3] H. Liu, Y. Du, Y. Deng, and P. D. Ye, "Semiconducting black phosphorus: synthesis, transport properties and electronic applications," *Chemical Society Reviews*, vol. 44, no. 9, pp. 2732–2743, 2015.

[4] J. Qiu, H. Fu, Y. Xu et al., "From silicene to half-silicane by hydrogenation," *ACS Nano*, vol. 9, no. 11, article 11192, 11199 pages, 2015.

[5] N. Youngblood, C. Chen, S. J. Koester, and M. Li, "Waveguide-integrated black phosphorus photodetector with high responsivity and low dark current," *Nature Photonics*, vol. 9, no. 4, pp. 247–252, 2015.

[6] T. Hu, Y. Han, and J. Dong, "Mechanical and electronic properties of monolayer and bilayer phosphorene under uniaxial and isotropic strains," *Nanotechnology*, vol. 25, no. 45, article 455703, 2014.

[7] J. Na, Y. T. Lee, J. A. Lim et al., "Few-layer black phosphorus field-effect transistors with reduced current fluctuation," *ACS Nano*, vol. 8, no. 11, pp. 11753–11762, 2014.

[8] Ø. Prytz and E. Flage-Larsen, "The influence of exact exchange corrections in van der Waals layered narrow bandgap black phosphorus," *Journal of Physics: Condensed Matter*, vol. 22, no. 1, article 015502, 2010.

[9] J. Kim, S. K. Baek, K. S. Kim, Y. J. Chang, and E. J. Choi, "Long-term stability study of graphene-passivated black phosphorus under air exposure," *Current Applied Physics*, vol. 16, no. 2, pp. 165–169, 2016.

[10] L. Li, Y. Yu, G. J. Ye et al., "Black phosphorus field-effect transistors," *Nature Nanotechnology*, vol. 9, no. 5, pp. 372–377, 2014.

[11] Z. Zhu and D. Tománek, "Semiconducting layered blue phosphorus: a computational study," *Physical Review Letters*, vol. 112, no. 17, article 176802, 2014.

[12] J. Xie, M. S. Si, D. Z. Yang, Z. Y. Zhang, and D. S. Xue, "A theoretical study of blue phosphorene nanoribbons based on first-principles calculations," *Journal of Applied Physics*, vol. 116, no. 7, article 073704, 2014.

[13] Y. Ding and Y. Wang, "Structural, electronic, and magnetic properties of adatom adsorptions on black and blue phosphorene: a first-principles study," *The Journal of Physical Chemistry C*, vol. 119, no. 19, pp. 10610–10622, 2015.

[14] M. Sun, Y. Hao, Q. Ren, Y. Zhao, Y. Du, and W. Tang, "Tuning electronic and magnetic properties of blue phosphorene by doping Al, Si, As and Sb atom: a DFT calculation," *Solid State Communications*, vol. 242, pp. 36–40, 2016.

[15] M. Sun, S. Wang, J. Yu, and W. Tang, "Hydrogenated and halogenated blue phosphorene as Dirac materials: a first principles study," *Applied Surface Science*, vol. 392, pp. 46–50, 2017.

[16] M. E. Dávila and G. le Lay, "Few layer epitaxial germanene: a novel two-dimensional Dirac material," *Scientific Reports*, vol. 6, no. 1, article 20714, 2016.

[17] M. Sun, W. Tang, Q. Ren, S. K. Wang, J. Yu, and Y. du, "A first-principles study of light non-metallic atom substituted blue phosphorene," *Applied Surface Science*, vol. 356, pp. 110–114, 2015.

[18] H. Zheng, H. Yang, H. Wang, X. du, and Y. Yan, "Electronic and magnetic properties of nonmetal atoms doped blue phosphorene: first-principles study," *Journal of Magnetism and Magnetic Materials*, vol. 408, pp. 121–126, 2016.

[19] J. Xiao, M. Long, C. S. Deng, J. He, L. L. Cui, and H. Xu, "Electronic structures and carrier mobilities of blue phosphorus nanoribbons and nanotubes: a first-principles study," *The Journal of Physical Chemistry C*, vol. 120, no. 8, pp. 4638–4646, 2016.

[20] L. Zhu, S. S. Wang, S. Guan et al., "Blue phosphorene oxide: strain-tunable quantum phase transitions and novel 2D emergent fermions," *Nano Letters*, vol. 16, no. 10, pp. 6548–6554, 2016.

[21] J. L. Zhang, S. Zhao, C. Han et al., "Epitaxial growth of single layer blue phosphorus: a new phase of two-dimensional phosphorus," *Nano Letters*, vol. 16, no. 8, pp. 4903–4908, 2016.

[22] C. Gu, S. Zhao, J. L. Zhang et al., "Growth of quasi-freestanding single-layer blue phosphorus on tellurium monolayer functionalized Au(111)," *ACS Nano*, vol. 11, no. 5, pp. 4943–4949, 2017.

[23] G. Kresse and J. Hafner, "*Ab initio* molecular dynamics of liquid metals," *Physical Review B*, vol. 47, no. 1, pp. 558–561, 1993.

[24] G. Kresse and J. Furthmüller, "Efficient iterative schemes for *ab initio* total-energy calculations using a plane-wave basis set," *Physical Review B*, vol. 54, no. 16, article 11169, 1996.

[25] J. P. Perdew, K. Burke, and M. Ernzerhof, "Generalized gradient approximation made simple," *Physical Review Letters*, vol. 77, no. 18, pp. 3865–3868, 1996.

[26] G. Kresse and D. Joubert, "From ultrasoft pseudopotentials to the projector augmented-wave method," *Physical Review B*, vol. 59, no. 3, pp. 1758–1775, 1999.

[27] P. E. Blöchl, "Projector augmented-wave method," *Physical Review B*, vol. 50, no. 24, article 17953, 1994.

[28] M. Aykol, J. W. Doak, and C. Wolverton, "Phosphorus allotropes: stability of black versus red phosphorus re-examined by means of the van der Waals inclusive density functional method," *Physical Review B*, vol. 95, no. 21, article 214115, 2017.

[29] T. Bučko, J. Hafner, S. Lebègue, and J. G. Ángyán, "Improved description of the structure of molecular and layered crystals: ab initio DFT calculations with van der Waals corrections," *The Journal of Physical Chemistry A*, vol. 114, no. 43, article 11814, 11824 pages, 2010.

[30] K. Parlinski, Z. Q. Li, and Y. Kawazoe, "First-principles determination of the soft mode in cubic $ZrO_2$," *Physical Review Letters*, vol. 78, no. 21, pp. 4063–4066, 1997.

[31] B. Ghosh, S. Nahas, S. Bhowmick, and A. Agarwal, "Electric field induced gap modification in ultrathin blue phosphorus," *Physical Review B*, vol. 91, no. 11, article 115433, 2015.

[32] S.-s. Li, W.-x. Ji, P. Li et al., "Unconventional band inversion and intrinsic quantum spin Hall effect in functionalized group-V binary films," *Scientific Reports*, vol. 7, no. 1, article 6126, 2017.

[33] Y.-p. Wang, W. X. Ji, C. W. Zhang et al., "Large-gap quantum spin Hall state in functionalized dumbbell stanene," *Applied Physics Letters*, vol. 108, no. 7, article 073104, 2016.

[34] H. Zhao, C. W. Zhang, W. X. Ji et al., "Unexpected giant-gap quantum spin Hall insulator in chemically decorated plumbene monolayer," *Scientific Reports*, vol. 6, no. 1, article 20152, 2016.

[35] R.-W. Zhang, C. W. Zhang, W. X. Ji et al., "Ethynyl-functionalized stanene film: a promising candidate as large-gap quantum spin Hall insulator," *New Journal of Physics*, vol. 17, no. 8, article 083036, 2015.

[36] C.-C. Ren, S. F. Zhang, W. X. Ji, C. W. Zhang, P. Li, and P. J. Wang, "Tunable electronic and topological properties of germanene by functional group modification," *NanoMaterials*, vol. 8, no. 3, p. 145, 2018.

[37] Y. P. Wang, W. X. Ji, C. W. Zhang et al., "Controllable band structure and topological phase transition in two-dimensional hydrogenated arsenene," *Scientific Reports*, vol. 6, no. 1, article 20342, 2016.

[38] C.-C. Ren, Y. Feng, S. F. Zhang, C. W. Zhang, and P. J. Wang, "The electronic properties of the stanene/$MoS_2$ heterostructure under strain," *RSC Advances*, vol. 7, no. 15, pp. 9176–9181, 2017.

[39] V. Wang, Y. C. Liu, Y. Kawazoe, and W. T. Geng, "Role of interlayer coupling on the evolution of band edges in few-layer phosphorene," *Journal of Physical Chemistry Letters*, vol. 6, no. 24, pp. 4876–4883, 2015.

[40] X. D. Zhang, M. L. Guo, C. L. Liu, L. A. Zhang, and W. Y. Zhang, "First-principles investigation of electronic and optical properties in wurtzite $Zn_{1-x}$ $Mg_xO$," *The European Physical Journal B*, vol. 62, no. 4, pp. 417–421, 2008.

[41] Y. Ding and Y. Wang, "Electronic structures of silicene/GaS heterosheets," *Applied Physics Letters*, vol. 103, no. 4, article 043114, 2013.

[42] Y. Feng, W. X. Ji, B. J. Huang et al., "The magnetic and optical properties of 3d transition metal doped $SnO_2$ nanosheets," *RSC Advances*, vol. 5, no. 31, pp. 24306–24312, 2015.

[43] F. Li, C. Zhang, and M. Zhao, "Magnetic and optical properties of Cu-doped ZnO nanosheet: first-principles calculations," *Physica E: Low-dimensional Systems and Nanostructures*, vol. 53, pp. 101–105, 2013.

[44] Y. Feng, B. J. Huang, S. S. Li et al., "Electronic structure and optical properties of Bi,N,co-doped $SnO_2$," *Journal of Materials Science*, vol. 50, no. 21, pp. 6993–6999, 2015.

[45] W.-b. Xu, B.-j. Huang, P. Li, F. Li, C.-w. Zhang, and P.-j. Wang, "The electronic structure and optical properties of Mn and B, C, N co-doped $MoS_2$ monolayers," *Nanoscale Research Letters*, vol. 9, no. 1, p. 554, 2014.

[46] B. J. Huang, F. Li, C. W. Zhang, P. Li, and P. J. Wang, "Electronic structure and optical properties of Ag-doped $SnO_2$ nanoribbons," *RSC Advances*, vol. 4, no. 79, pp. 41819–41824, 2014.